CHAPTER - VII

Electrochemical Properties of Mn - Oxide Films.

CHAPTER - VII

ELECTROCHEMICAL PROPERTIES OF Mn-OXIDE FILMS

7.1 Introduction :

In many semiconductors, recently electrochemical characterisation has been used successfully to determine the band-gap, doping density, space charge layer width, absorption coefficient, type of conductivity, composition, diffusion length of minority carriers etc. /1/. The use of semiconductor electrodes as intermediates for solar energy conversion has been recently the subject of intensive research /2-6/. The electrochemical characterisation can be done with the help of ECPV cells. The theory of the ECPV cells has been reviewed by many authors /7-14/. In this chapter construction of ECPV cell, experimental setups for electrical characterisation are described and the effect of concentration of spraying solution on Mott-Schottky plot is discussed.

7.2 Electrochemical Photovoltaic Cell : General Background :

An ECPV cell consists of a semiconductor photoelectrode, an electrolyte and a counter electrode. All these parts play an important role in the ECPV cell. A Schotkky type of cell was constructed in which one electrode was a photoactive semiconductor and the other a metallic counter electrode.

Semiconductor photoelectrode being heart of the ECPV cell, any modification in the properties of a semiconductor photoelectrode reflects consecutive changes in the electrical properties of a cell. It has certain advantages over the

metals as higher quantum efficiency for electron flow, longer life time of the photogenerated electron-hole pairs, potential drop occurs in the depletion layer and not in the Helmholtz double layer and allows considerable scope for doping, surface treatment etc. In general photoelectrode used in ECPV cell should satisfy the following requirements:

1) The bandgap (E_g) of the photoelectrode material should match with the maximum span of the solar spectrum i.e. $E_g \simeq 1.4$ to 1.6 eV.

2) It should be stable in the electrolyte and should not decompose during illumination.

3) It should be of the direct bandgap type with high optical absorption coefficient (10^4 to 10^5 cm^{-1}).

4) Charge carriers in the material should have high mobility and life time.

5) Thickness of the material should be large enough to absorb all the incident radiations, and

6) Cost of the material and manufacturing process and efficiency should be acceptable.

An electrolyte plays an equally important role in the ECPV cell, which helps to scavage the photogenerated holes from photoelectrode to counter electrode. The energy levels in the electrolyte are analogous to the concept of energy states in a solid and E_F, redox is equivalent to the Fermi

energy of a semiconductor. As the difference between E_F of a semiconductor and $E_{F\ redox}$ of an electrolyte defines the upper limit to photovoltage, the choice lies both for semiconductors and electrolytes. It is observed that aqueous electrolytes cause surface modifications and hence restrict the use of many semiconductors. Molecular organic or inorganic solvents with supporting electrolytes and mixtures of totally ionic molten salts have been substituted for aqueous electrolytes /15-17/.

A counter electrode is a third essential part of an ECPV cell. In a regenerative process the electrolyte species are oxidized at the photoanode and are again reduced at the counter electrode giving no net chemical change in the composition of an electrolyte. Requirements of counter electrode for use in ECPV cell are /18/ (a) it should be chemically inert i.e. it should not form any new compound by reacting with electrolyte, otherwise, it will change the electrolyte composition as well as counter electrode properties, (b) it should be non-polarizable electrode means that it should allow free and unimpeded exchange of electrons or ions across the semiconductor-electrolyte interface /19/. When a charge crosses an ideal reversible electrode, the electrochemical change takes place with such a rapidity that the equilibrium situation is restored instantaneously. Thus a non-polorised counter electrode will allow all the applied voltage to appear

across the semiconductor-electrolyte interface, (c) it should have low overpotential for reduction reaction. In the ECPV cells, platinum in the form of wire or foil and carbon in the form of rod or plate are used as counter electrodes as they fulfil first two requirements /20-22/. Also silver sulfide and gold are used as counter electrode. Hodes et al. /23/ have shown that the use of high surface area spectroscopic grade carbon rods treated with cobalt sulfide (CoS) gives much better performance than platinum, silversulfide or gold in aqueous redox electrolyte.

7.3 Experimental Details :

7.3.1 Construction of ECPV cell

The Mn-oxide thin film photoelectrodes were deposited on conducting and non-conducting glass substrates at various deposition temperatures by using spray pyrolysis technique as described in Chapter III.

The potassium ferro and ferri cyanide [K_4/K_3 $Fe(CN)_6$] redox system with NaOH as supporting electrolyte and their composition 0.5 M NaOH + 0.01 M K_4 $Fe(CN)_6$ + 0.01 M $K_3Fe(CN)_6$ were prepared in double distilled water and well filtered before use.

Carbon rods of the size 4 cm length and 0.5 cm diameter was used as counter electrode. Considering all above three parts, an ECPV cell was constructed by employing polycrystalline Mn-oxide as a photoelectrode, carbon rod as a counter

electrode and a Ferro/Ferri cyanide as a redox system with NaOH as a supporting electrolyte.

The ECPV cell has following configuration :

Mn-oxide/0.5 NaOH + 0.01 M [K_4/K_3 $(Fe(CN)_6)$] / C

The distance between the photocathode and the counter electrode was 2 mm. The length from the window of the cell to the Mn-oxide photoelectrode was about 0.5 cm. The photoelectrode was irradiated with light from 500 watt tungston filament lamp. The intensity of light at the cell window was 100 mW/cm^2 and was measured with a calibrated 'Suryamapi' (Aplab Luxmeter).

The design of an ECPV cell is shown in fig.7.1 which consists of a modified corning tube, fixed inside a copper calorimeter having a window of size 2 x 0.7 cm^2 for illumination of the photoelectrode. A rubber cork was used to air-tight the cell. A saturated calomel electrode can be used in another tube of the cell.

7.3.2 Experimental setups for Electrical Characterization of ECPV Cell

The electrical characterization of an ECPV cell is necessary to get the knowledge about the charge transfer processes across the semiconductor-electrolyte interface. The experimental setups for electrical studies of an ECPV cell are described below.

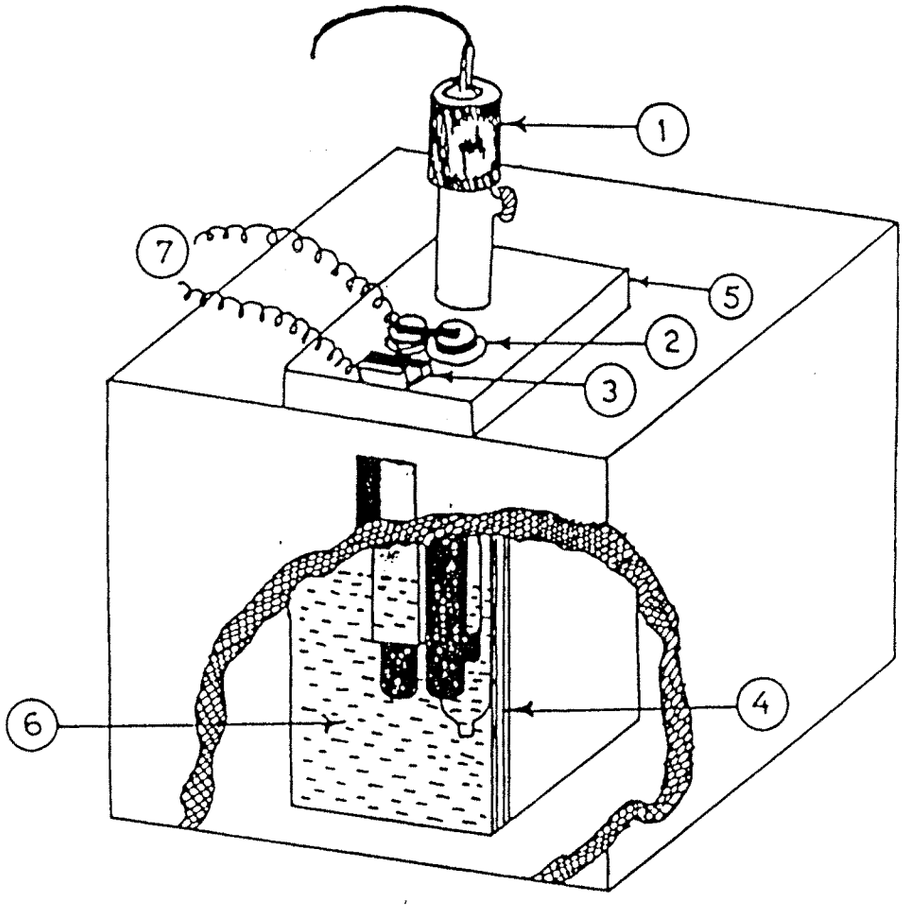

Fig. 7.1 Schematic diagram of electrochemical photovoltaic cell.
1) Standard Calomel electrode (SCE)
2) Counter electrode 3) Photocathode
4) Quartz window 5) Holder for electrodes
6) Electrolyte 7) Cell terminals.

i) Current-voltage characteristics in dark and in light :

The circuitry used for the study of I-V characteristics in the dark and under illumination is shown in fig.7.2. A ten turn potentiometer (5kΩ) was used to vary the potential applied to the cell. The current through the circuit and voltage applied to the cell were measured by a Aplab FET input nanometer TFM-13 and a high input impedance digital pla panel voltmeter DPM-10 respectively. A 500 watt tungsten filament lamp was employed to illuminate the cell. A water filter was interposed between the lamp and the cell to avoid heating of the cell. The experimental set-up is shown in fig. 7.3.

ii) Capacitance-Voltage characteristics :

The capacitance-voltage (versus SCE) measurements in the dark under reverse bias condition were carried out by a potentiometric arrangement as shown in fig.7.4. A photograph of the experimental setup for C-V measurement is shown in fig. 7.5. The potential applied to the junction was varied by a ten turn (5kΩ) potentiometer and was measured by a Pla digital d.c. voltmeter DPM-10. The junction capacitance per unit area at various junction voltages with respect to SCE were recorded by a digital display capacitance meter VCM-13A, at 1 KHz frequency.

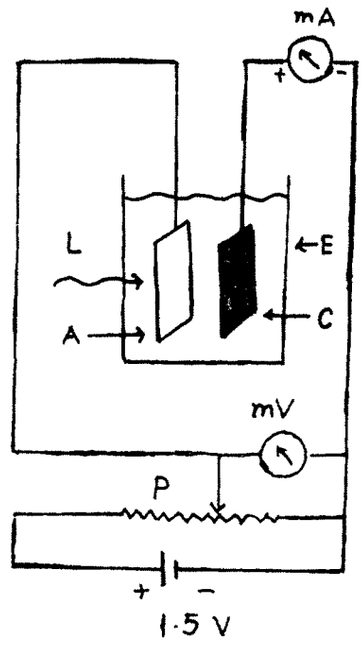

E - ECPV Cell , C - Counter electrode , A - Photocathode,
P - Potentiometer , L - Light , mA - milliammeter, mV - Millivoltmeter

Fig. 7.2 Circuit diagram for current voltage characteristics of the ECPV cell.

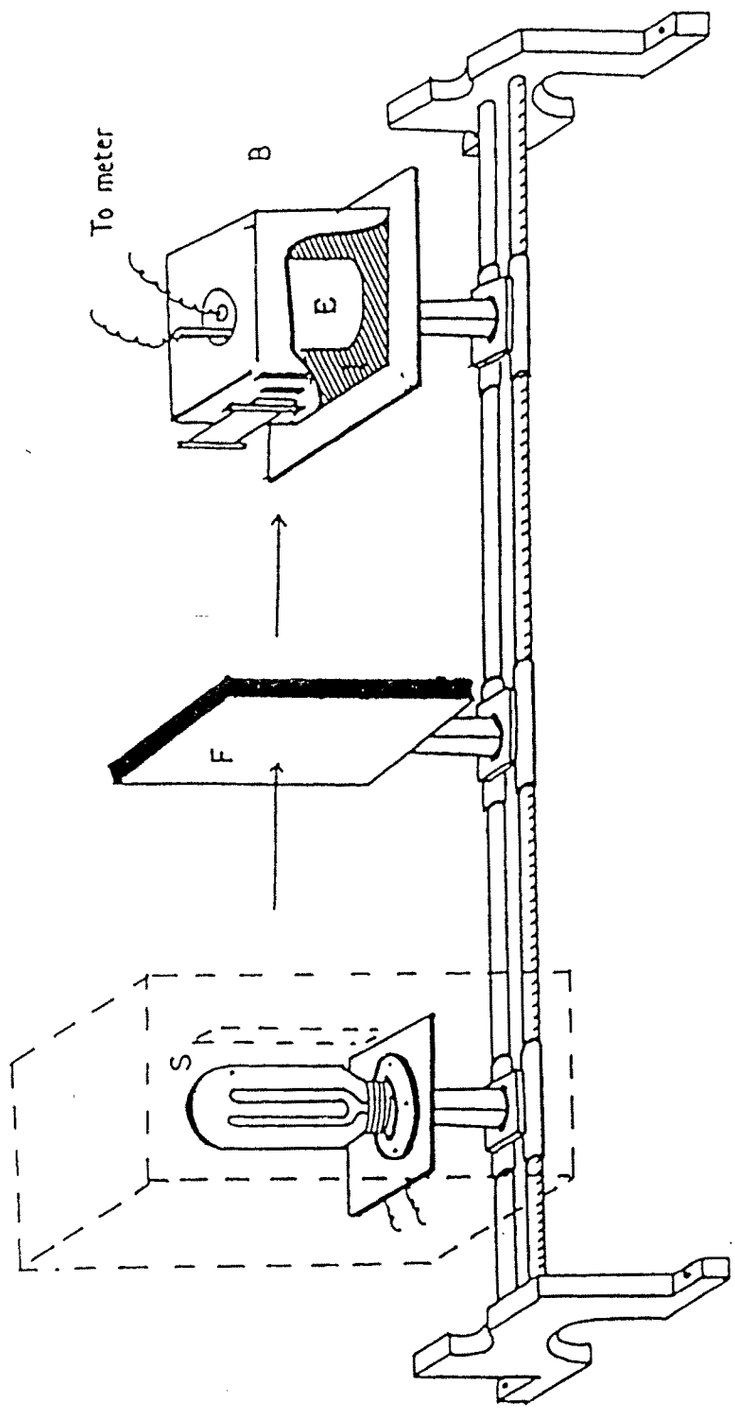

S - Light source , B - Bakelite box , ECPV cell - E ,
I - Insulator , O - Optical bench , F - Water filter .

Fig. 7.3 Experimental set-up for I-V characteristics in light.

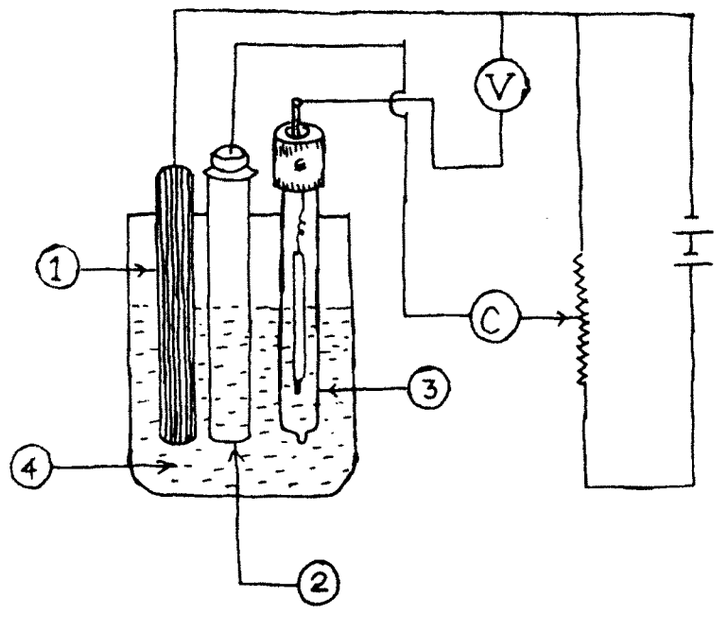

Fig. 7.4 Circuit diagram for capacitance-voltage measurement of the ECPV cell.

1) Photocathode 2) Counter electrode

3) SCE and 4) Electrolyte.

Fig. 7.5 Photograph of experimental setup of C-V measurement of an ECPV cell.
1) Cell with backelite box 2) Capacitance meter
3) Potentiometric arrangement 4) Voltmeter.

7.4 Results and Discussion :

The Mn-oxide film which was deposited at 400°C substrate temperature by spraying manganese chloride solution of 0.25 M concentratiion is used as a photoelectrode in ECPV cell to study type of conductivity and I-V characteristics.

7.4.1 Type of Conductivity

The open circuit voltage of the photoelectrochemical system Mn-oxide/0·5 M NaOH + 0·01 M K_4/K_3 $Fe(CN)_6$/C was measured at 100 mW/cm^2 illumination intensity. The photovoltage sign gives the conductivity type of semiconductor electrode /1,24/. In this system cathodic behaviour of the photovoltage of the semiconductor was observed which indicates p-type conductivity. This result agrees well with that obtained from thermoelectric power measurement.

7.4.2 Current-Voltage Characteristics

When a semiconducting film of the Mn-oxide was dipped into an electrolyte a dark voltage V_D and dark current I_D were observed. The polarity of the dark voltage V_D is positive towards the carbon electrode. The origin of the dark voltage is attributed to the difference between half cell potentials of the photoelectrode and the carbon electrode and can be written as /25/

$$E = E_{carbon} - E_{Mn\text{-}oxide} \qquad \ldots (7.1)$$

where E_{carbon} and $E_{Mn\text{-}oxide}$ are half cell potentials developed when carbon and Mn-oxide electrodes are introduced in

the electrolyte. From the observed polarity of the voltage it is seen that

$$E_{carbon} < E_{Mn\text{-}oxide} \qquad \ldots (7.2)$$

The presence of dark current I_D in the cell suggests that there is some deterioration of the photoelectrode in dark.

In order to understand the charge transfer process across semiconductor-electrolyte interface. The current-voltage (I-V) characteristics of the cell p-Mn-oxide/0.5 M NaOH + 0.01 M K_4/K_3 $Fe(CN)_6$/C is studied. Fig.7.6 shows the I-V characteristics for the Mn-oxide based ECPV cell. It is seen that the forward current increases rapidly with applied bias. The increase of forward current can be attributed to the small contact barrier height and increase in tunneling mechanism /26,27/. Current in reverse bias does not saturate but increases slowly with an applied bias. In an electrode-electrolyte system, the nature of the charge transfer across the junction is given by the Butler-Volmer equation /19,28/ as :

$$I = I_o \left[e^{(1-\beta)VF/RT} - e^{-\beta VF/RT} \right] \qquad \ldots (7.3)$$

where I_o is equilibrium exchange current density, β is the symmetry factor, V is the overvoltage, R is the universal gas constant and F is the Faraday constant. For voltage > 100 mV, equation (7.3) can be written as

$$I = I_o \left[e^{(1-\beta)VF/RT} \right] \qquad \ldots (7.4)$$

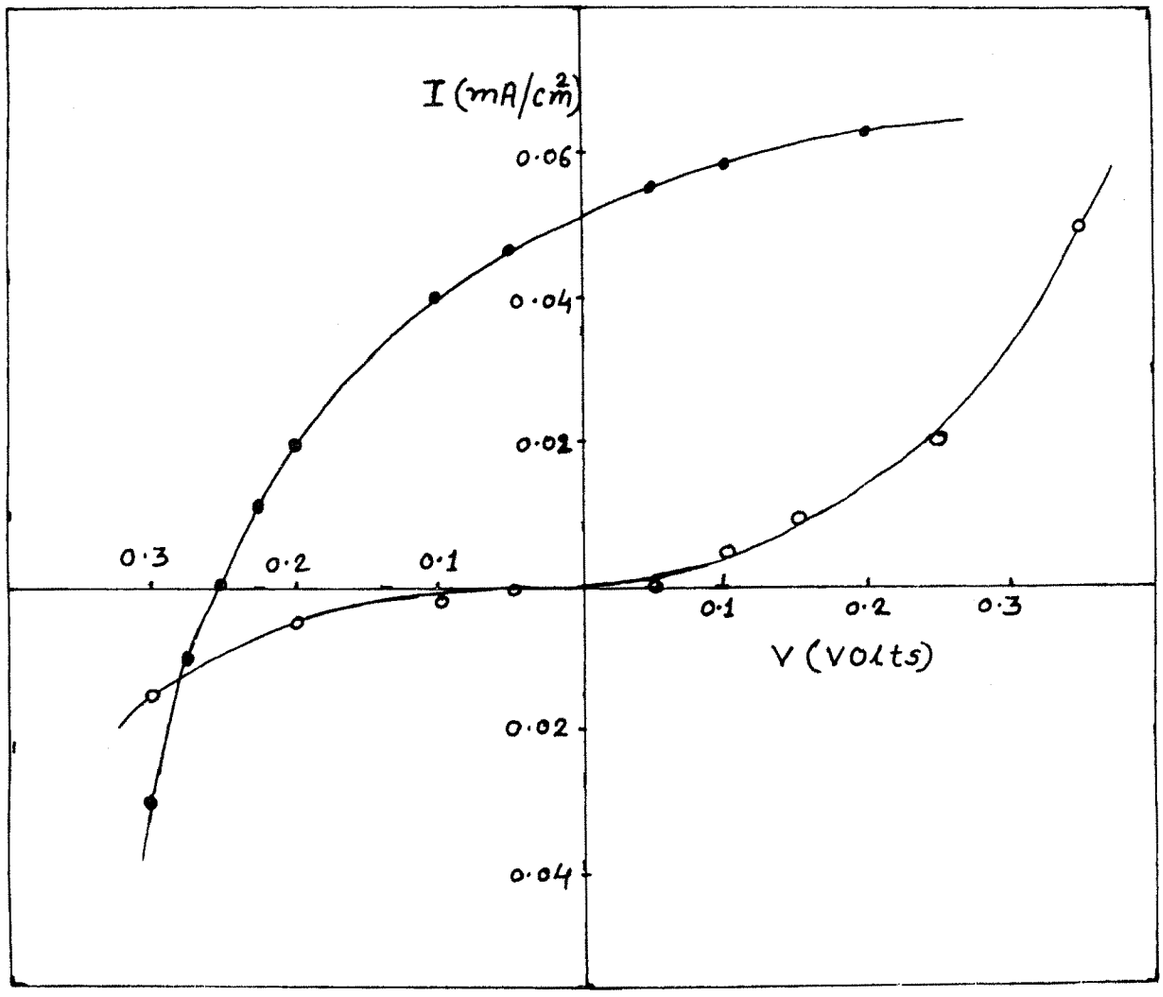

Fig. 7.6 Dynamic current-voltage characteristics in the dark and light for the ECPV cell.

when β is equal to 0.5, equation (7.3) becomes

$$I = I_o \left[e^{+FV/2RT} - e^{-FV/2RT} \right] \quad \ldots (7.5)$$

and this can be further expressed as

$$I = 2I_o \sinh (FV/2RT) \quad \ldots (7.6)$$

The I versus sinh V curve is symmetrical. A symmetry factor of 0.5 corresponding to a symmetrical barrier yields a symmetrical I versus V curve. This means that the interface cannot rectify a periodically varying potential or current. If $\beta \neq 0.5$, then the I versus V curve would not be symmetrical and the interface has rectifying properties. This is known as Faradic rectification /29/. The non-symmetrical nature of the I-V curve in the forward and reverse bias configuration observed in fig.7.6 shows that the junction formed in the ECPV cell is a rectifying one and identical to a Schottky barrier junction.

Dynamic I-V curve under illuminatioin was recorded by using a variable D.C. power supply in series with the external circuit and is shown in fig.7.6. When the cell is exposed to light, the I-V curve is shifted into the second quadrant indicating thereby the cell formed with Mn-oxide photocathode is a generator of electricity. This is in accordance with the standard results of ECPV cells /30/.

Fig. 7.7 shows photovoltaic power output curve for a typical cell, under an illumination intensity of 100 mW/cm^2.

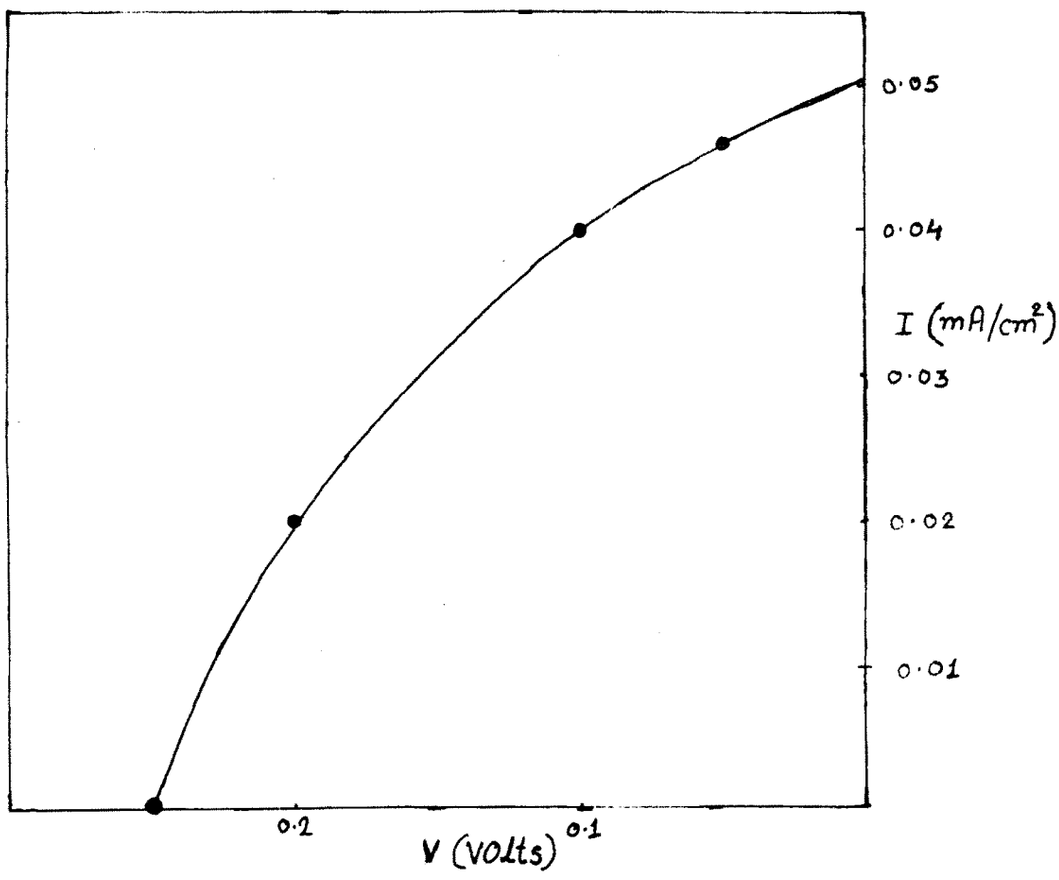

Fig. 7.7 Photovoltaic power output curve.

Efficiency of the cell, η , and fill factor, ff, were determined from this curve.

The photovoltaic devices are threshold devices i.e. they require a minimum optical energy to activate them. The energy conversion efficiency (η) of any threshold device is given by /8,31/.

$$\eta = \frac{E_{stor} \int_{Eth} \alpha(E)\, \phi_o(E)\, dE}{E \int \phi_o(E)\, dE} \qquad \ldots (7.7)$$

where Eth is the bandgap of the semiconductor, $\phi_o(E)$ is the number of photons with energy E, $\alpha(E)$ is the fraction of photons absorbed and E_{stor} is cell voltage. An inspection of equation 7.7 indicates that the efficiency would be larger if:

(a) the bandgap is high. However, it may be noted that the photodecomposition of semiconductor electrodes limits the conversion efficiency to a maximum of $(E_C - E_D)/E_g$ where E_D is the decomposition energy.

(b) $\alpha(E)$ is high. The expression for $\alpha(E)$ near the band edge is approximately written as

$$\alpha(E) = \frac{A\,(h\nu - Eg)^{n/2}}{h\nu} \qquad \ldots (7.8)$$

where A is a constant and n=4 for indirect bandgap. Hence the value of Eg should be small. Both these conditions are in contradiction with each other. Thus η , of expression 7.7 would be maximum for some optimum value of Eg.

In addition to Eg, there are other factors also which affect the efficiency of ECPV cell. These are as follows/8/: (i) physical properties of the semiconductor, (ii) energy losses due to the photoinduced redox reactions (iii) light losses due to absorption in the electrolyte, reflection from semiconductor surface etc., (iv) ohmic losses due to absorption in the electrolyte, semiconductor etc., (v) losses due to concentration polarisation if the redox process is slow.

The optical to electrical energy conversion efficiency in a semiconductor/liquid junction cell is given by /12/

$$\eta = \frac{(I.V)_{max}}{P_{input}} \times 100\ \% \qquad \ldots (7.9)$$

where $(I.V)_{max}$ is the maximum output power.

A parameter namely, fill factor, ff is defined as

$$ff = \frac{(I.V)_{max}}{I_{sc} \cdot V_{oc}} \qquad \ldots (7.10)$$

where I_{sc} and V_{oc} are short circuit photocurrent and open circuit voltage respectively.

Using equations (7.9) and (7.10) the energy conversion efficiency and fill factor are calculated from the photovoltaic power output curve as shown in fig.7.7. The calculated efficiency (η) is 0.005 % and fill factor is 38.4%. The poor efficiency may be due to losses as explained previously or due to improper redox system.

The value of dark ideality factor n_d is determined by plotting the graph of log I versus V shown in fig.7.8 which yields straight line. The value of n_d calculated using slope is 3.50. It is seen that, the value of n_d is high and this higher value can be attributed to the degree of recombination of charge carriers in the depletion region and is indicative of non-ideal junctions /32/.

7.4.3 Capacitance-Voltage Characteristic

The study of C-V characteristic is the measurement of interface capacitance with applied bias. Fig.7.5 shows the experimental arrangement for C-V characteristic study. Mn-oxide film deposited by spray pyrolysis was oneelectrode, carbon was used as the counter electrode and a saturated calomel electrode (SCE) was the third electrode, SCE was kept near the Mn-oxide film. The NaOH electrolyte had the redox couple K_4/K_3 $Fe(CN)_6$.

The flat band potential V_{fb} of a semiconductor is an important factor in explaining the C-V behaviour and charge transfer process across the semiconductor-electrolyte junction of a ECPV cell in dark /33/.

In case of the ECPV cell the measured capacitance is not only the capacitance due to depletion layer but also a capacitance contributed by Helmholtz layer (C_H) and Gouy diffusion layer (C_D). Since these two capacitances C_H and C_D are connected in series /11,19,28,34,35/.

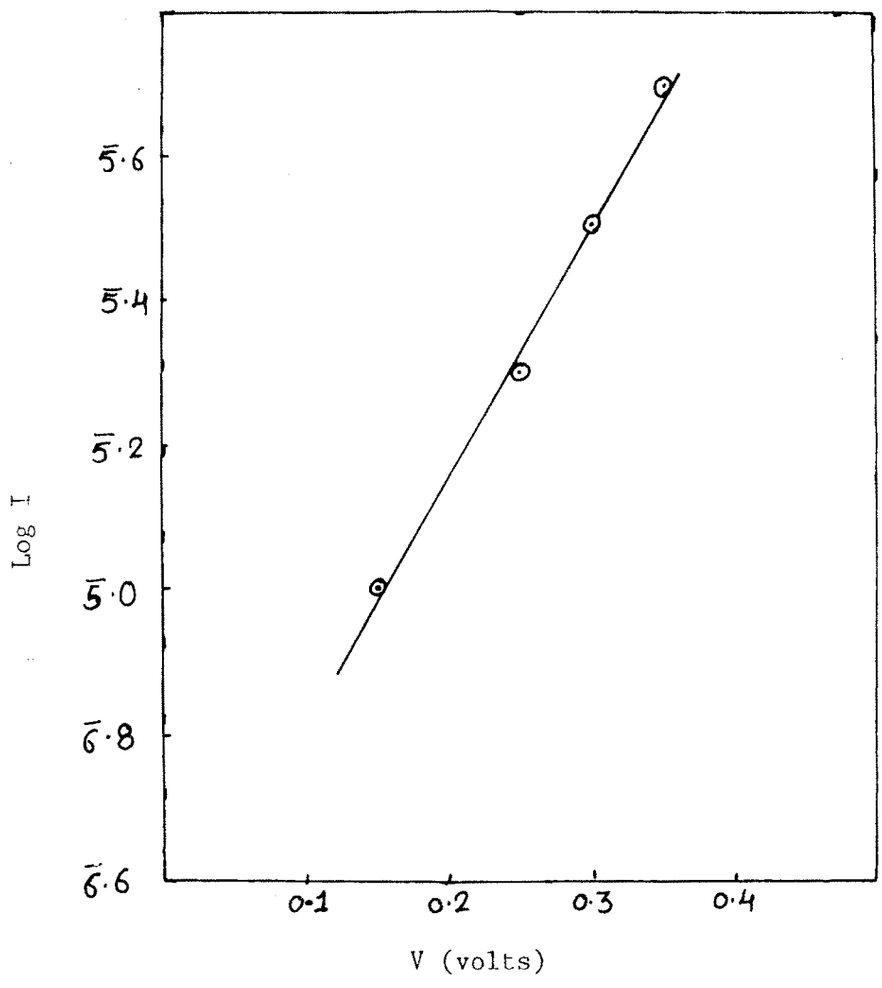

Fig. 7.8 Plot of log I versus V.

$$\frac{1}{C} = \frac{1}{C_H} + \frac{1}{C_D} \qquad \ldots (7.11)$$

The series capacitance of semiconductor-electrolyte junction is shown in fig. 7.9. Where C_{sc} is the capacitance due to semiconductor space charge region and C_{ss} is the capacitance due to surface states. In the present study capacitance due to Helmholtz and Gouy diffusion layers are neglected by considering high ionic concentration of the electrolyte. Using the above assumption one can express the flat band potential V_{fb} /36/ as :

$$C^{-2} = \frac{2}{q\epsilon\epsilon_o N_D} \left(V - V_{fb} - \frac{KT}{q} \right) \qquad \ldots (7.12)$$

where V_{fb} is the flat band potential equal to the bias which makes the band bending zero, ϵ is the dielectric constant of the semiconductor, ϵ_o is the permittivity of free space, q is the electronic charge and N_D is the doping density. The above equation shows that the plot of C^{-2} versus V should be a straight line. This plot is known as Mott-Schottky plot. The intercept of the linear plot to the voltage axis at $C^{-2}=0$ offered a quantitative measure of the electrode potential of flat band condition /29/. Further from the slope of the straight line the value of N_D can be calculated.

Fig. 7.10 shows the Mott-Schottky plot of the Mn-oxide film deposited at 400°C substrate temperature dipped in NaOH electrolyte having redox couple K_4/K_3 $Fe(CN)_6$. The nature of

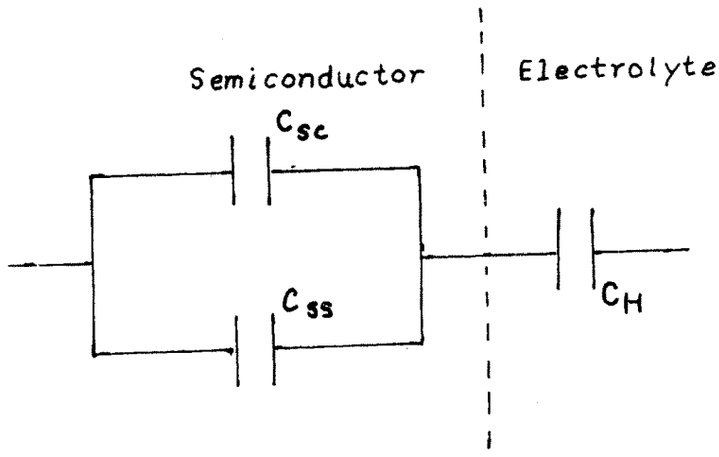

Fig. 7.9 Equivalent circuit diagram of capacitance formed at S-E interface.

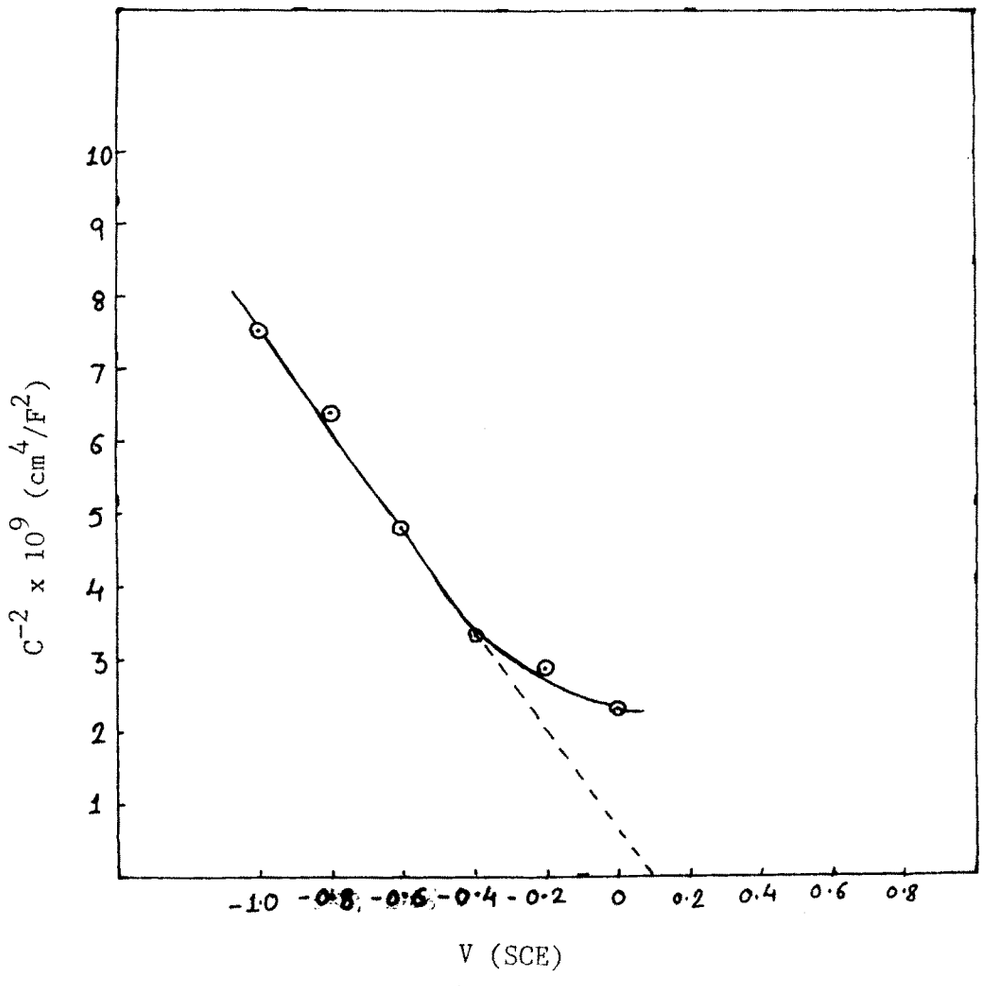

Fig. 7.10 Mott-Schottky plot for the ECPV cell

the plot indicates that film is P-type /37/. The values of flat band potential and acceptor density were obtained as 0.1 V and 4.4 x 10^{21} cm^{-3}. The dielectric constant for semiconductor, which was obtained from the ellipsometric calculation is used to calculate acceptor density. The dielectric constant for the typical semiconductor (Mn-oxide) was found to be 2.67. Fig. 7.11 shows the Mott-Schottky plots for the film prepared with different concentration of spraying solution. The plots show that there is change in flat band potential with concentration.

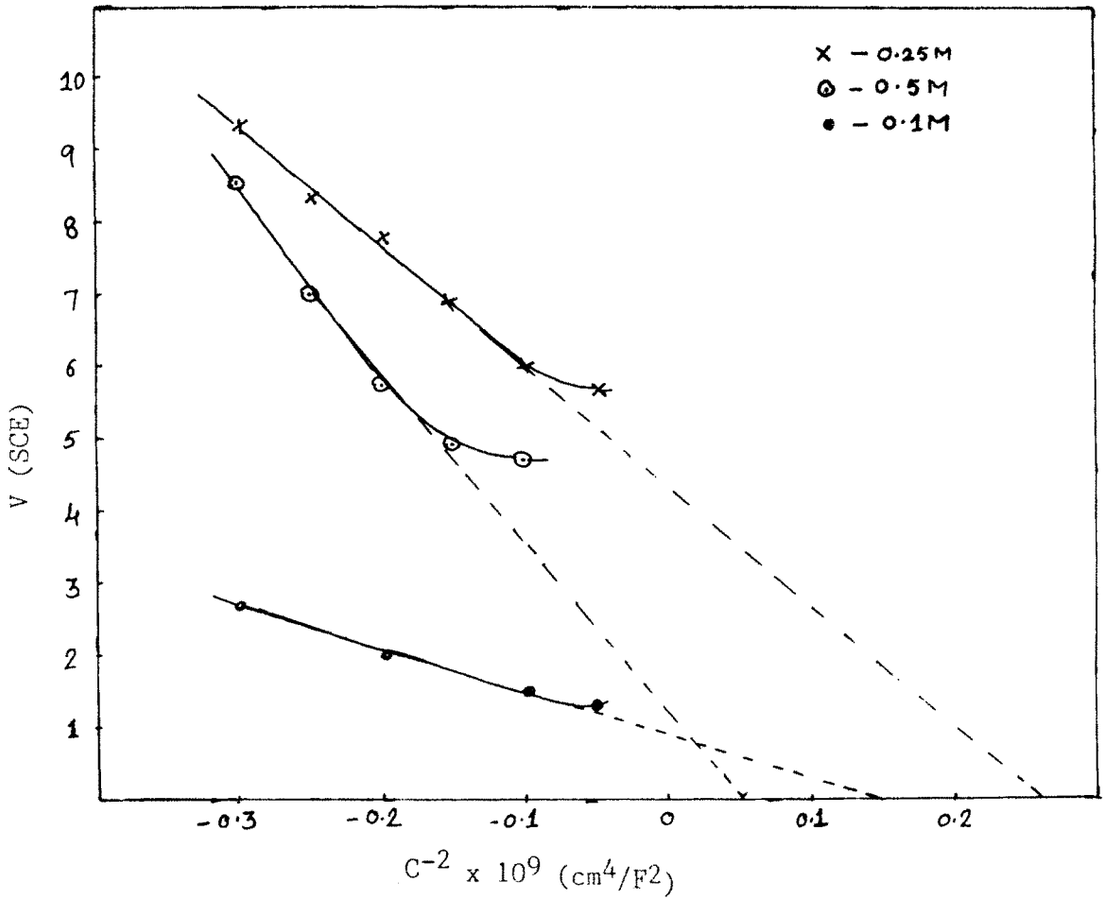

Fig. 7.11 Mott-Schottky plots for the films prepared with different concentration of spraying solution.

REFERENCES

1. M.M.Factor, T.Ambridge, C.R.Elliot and J.C.Ragnault, 'Current Topics in Material Science' ed. E.Kaldis (Amsterdam North Holland) vol.6 (1980). p.1.
2. M.Ftaman, J. Phys. Chem., 90, 1844 (1986).
3. B.L.Wheeler, J.K.Leland and A.J.Bard, J.Electrochem. Soc., 133, 358 (1986).
4. R.C.Kainthla, B.Zelenay and J.O'M. Bockrij, J. Electrochem. Soc. 133, 248 (1986).
5. W.M.Shen, W.Siripala, M.Tomkiewicz and D.Cahen, J.Electrochem. Soc., 133, 107 (1986).
6. R.Tenne and A.Wold, Appl. Phys. Letts., 47, 707(1985).
7. H.Gerischer in 'Topics in Applied Physics Vol.31', ed.B.O.Seraphin, Springer, Berlin-Heidelberg (1979) p.115.
8. S.Chandra and R.K.Pandey, Phys.Stat.Sol. (0), 72, 415 (1982).
9. E.Buhks and F.Williams, Denver meeting. Electrochem. Soc. Inc. (1981).
10. R.Memming, Electrochimica Acta, 25, 77 (1980).
11. H.Gerischer, Pure and Appl. Chem. 52, 2449 (1980).

12. A.Aruchamy, G.Aravamudan and G.V.Subba Rao, Bull. Mater. Sci., 5, 483 (1982).

13. E.M.Elsenberg and H.P.Silvfrman, Electrochimica Acta, 5, 1 (1961).

14. A.P.B.Sinha and S.K.Date in 'Physics of Semiconductors' ed. S.Guha, Indian Physics Association (1982) P.137.

15. R.J.Gale and J.Dubow, Solar Energy Materials, 4, 135 (1981).

16. A.Hammet and S.Dennison, Nature 300, 687 (1982).

17. E.Plumat, F.Toussaint and M.J.Boffe, Am.Chem.Soc., 49, 551 (1966).

18. C.H.Bhosale, Ph.D.Thesis, Shivaji Univ., Kolhapur (1987).

19. D.R.Crow, 'Principles and Applications of Electrochemistry'. Chapman and Hall, London (1974).

20. M.Tsuiki, H.Minoura, T.Nakamura and Y.Ueno, J.Appl. Electrochem. 8, 523 (1978).

21. S.Chandra, R.K.Pandey and R.C.Agrawal, J.Phys. D, 13, 1757 (1980).

22. A.Heller, K.C.Chang and B.Miller, J.Electrochem. Soc., 124, 697 (1977).

23. J.Manassen, G.Hodes and D.Cahen, in 'Semiconductor-liquid junction solar cells', ed.A.Hellar, The Electrochem.Soc. Inc. Princeton (1977) p.34.

24. M.Peter, J.Electroanal. Chem. Interf. Electrochem., 144, 315 (1983).

25. C.D.Lokhande, Ph.D.Thesis, Shivaji Univ. Kolhapur (1983).

26. K.Rajeshwar, L.Thopson, P.Sing, R.C.Kinthia and K.L.Chopra, J.Electrochem.Soc., 128, 1744 (1981).

27. R.Williams, J.Electrochem.Soc., 114, 1173 (1967).

28. J.O'm Bockris and A.K.N.Reddy, "Modern Electrochemistry Vol.2, A Plenum/Rosetta edition, Chapter 7 (1973).

29. J.O'm. Bockris and A.K.N.Reddy, "Modern Electrochemistry" vol.2, A Planum/Rosetta edition Chapter 8 (1973).

30. J.Reichman and M.A.Russak in, "Photo effects at Semiconductor-Electrolyte Interface," ed. A.J.Nozik, ACDS, Sym. 146 (1981) p.359.

31. H.Gerischer in, "Semiconductor-liquid junction Solar cells," ed. A.Hellar. The Electrochem.Soc. Inc. Princeton, N.J. (1977), p.1.

32. H.J.Hovel, in "Semiconductors and semi-metals," ed. A.Beer and R.Willardson, Academic Press, New York (1975) p.86.

33. G. Hodes, Nature, 29, 284 (1980).

34. J.F.McCann and S.P.S. Badwal, J. Electrochem. Soc. 129, 521 (1982).

35. S.Chandra in 'Energy Resources Through Photoelectrochemical Routes", ed. S.H.Pawar, Ved Mitra and B.Venkataraman (1988).

36. R.Tene and G.Hodes, Appl. Phys. Letts., 37, 428 (1980).

37. H.Yoneyama, H.Sakamoto and H.Tamura, J.Electrochem. Acta, 20, 341 (1975).